

## Overexpression of BMP9 promotes ovarian cancer progression via Notch1 signaling

Lijuan YANG<sup>1,2</sup>, Yingying BAI<sup>1</sup>, Chaihong ZHANG<sup>1</sup>, Junhong DU<sup>1</sup>, Yuemei CHENG<sup>1</sup>, Qinganzi WANG<sup>1</sup>, Bo ZHANG<sup>3</sup>, Yongxiu YANG<sup>4\*</sup>

<sup>1</sup>The First Clinical Medical College of Lanzhou University, Key Laboratory of Gynecological Oncology of Gansu Province, Lanzhou, Gansu, China; <sup>2</sup>Molecular Oncology Laboratory, Department of Orthopedics Surgery and Rehabilitation Medicine, The University of Chicago Medical Center, Chicago, Illinois, United States; <sup>3</sup>Department of Orthopedics, Henan Provincial People's Hospital, People's Hospital of Zhengzhou University, Zhengzhou, Henan, China; <sup>4</sup>Department of Obstetrics and Gynecology, The First Affiliated Hospital of Lanzhou University, Key Laboratory of Gynecological Oncology of Gansu Province, Lanzhou, Gansu, China

\*Correspondence: yongxiuyang1964@163.com

Received March 26, 2021 / Accepted June 18, 2021

Cell proliferation and migration play important parts in ovarian cancer progression. BMP9, as one of the members of the TGF- $\beta$  superfamily and BMP family, plays a diverse and significant array of biological roles, including cell differentiation, proliferation, apoptosis, tumorigenesis, and metabolism. However, the role and mechanism of BMP9 in ovarian cancer progression remains uncertain. We found that the expression of BMP9 was increased in human ovarian cancer cell lines, which induced Notch1 intracellular domain (NICD1) accumulation. And we also found the expression abundance of BMP9 is low in ovarian cancer cells. Thus, we generated recombinant adenoviruses overexpressing BMP9 to perform the research. We found that overexpression of BMP9 promoted ovarian cancer cell proliferative viability, cell cycle progression, cell migration *in vitro*, and accelerated subcutaneous tumor growth *in vivo*, which was inhibited by dominant-negative mutant Notch1 recombinant adenoviruses. Besides, we also demonstrated that silencing of BMP9 by recombinant adenoviruses inhibited ovarian cancer cell viability and migration *in vitro*. Additionally, BMP9-induced ovarian cancer cell progression also involved the elevation of HES2, c-Myc, MMP9, and Cyclin D1, as well as repressed expression of p27. Together, these results revealed that BMP9 acts as a promoting factor in ovarian cancer progression, and overexpression of BMP9 promotes ovarian cancer progression and growth via Notch1 signaling. Thereby our research may provide new insight into the pathogenesis of ovarian cancer and BMP9-Notch1 signaling may serve as a novel therapeutic target axis for ovarian cancer treatment.

*Key words: ovarian cancer, BMP9, growth, progression, Notch1 signaling*

Ovarian cancer (OC) is a multistep disease in which numerous basic processes, including cell proliferation, migration, division, and apoptosis, are dysregulated [1]. Unfortunately, these processes remain unclear, which contributes to the unsatisfactory therapeutic effect of OC [2]. Cell proliferation and migration are regarded to play crucial roles in elucidating the pathogenesis of OC. And potential treatment targets will be found in the research of OC [3–6].

Bone morphogenetic protein 9 (BMP9, also known as GDF2) is one of the most promising members of the BMPs family, which participates in regulating cell proliferation, migration, motility, and adherence [7]. However, the role and mechanism of BMP9 in OC cell proliferation and migration have remained uncertain. Herrera et al. [8] found that BMP9 facilitated the proliferation of human ovarian epithelial cells and OC cells via the ALK2/Smad1/Smad4 pathway using siRNA targeting BMP9 and BMP9 reagent *in vitro*.

However, Varadaraj et al. [9] indicated that BMP9 played an anti-metastatic role in OC and BMP9 did not have a pro-proliferative role in ovarian epithelial cells, and BMP9 promoted ovarian epithelial cell anoikis via the ALK3/ALK6/SMAD1/5 signaling *in vitro*. Consequently, the function of BMP9 in OC remained ambiguous. It is known that the level of BMP9 is medium or low in OC tissues. Accordingly, we constructed recombinant adenoviruses overexpressing or silencing human BMP9 to clarify the role of BMP9 in OC progression through *in vivo* and *in vitro* experiments.

Notch signaling pathway contains four receptors (Notch1, 2, 3, 4), five ligands (Dll1, 3, 4, and Jag1, 2), regulators, and transcription factors in mammals [10]. Notch protein releases active Notch intracellular domain (NICD) from the membrane in two steps by a Disintegrin and Metalloprotease (ADAM) and  $\gamma$ -secretase, and NICD functions directly in the signal transmission through interacting with the transcrip-

tion factor CSL to regulate downstream target genes such as hairy and enhancer of split (HES) family into the nucleus. It was shown that the Notch signaling pathway plays a critical role in a wide range of biological processes including tumorigenesis [10–13]. However, it remains unclear whether BMP9 participates in OC progression through the Notch signaling.

Currently, the effect of BMP9 on ovarian cancer cell proliferation remains an area of substantial controversy. The relationship between BMP9 and Notch1 in OC cell proliferation and migration remains unclear. Hence, the aim of our study was to clarify the specific mechanisms underlying BMP9-Notch1 signaling-mediated proliferation and migration of OC cells. Accordingly, we constructed recombinant adenoviruses overexpressing BMP9 or dominant-negative Notch1 to perform subcutaneous tumor formation assay and *in vitro* experiments. Our study may provide useful information for OC treatment.

## Materials and methods

**Cell culture.** Immortalized human ovarian surface epithelial cell (IOSE364), human ovarian cancer lines (SKOV3, HeyA8, CAOV3, OVCAR3, OVCAR8), and HEK-293 were kindly provided by T.-C. He, MD, PhD. from the University of Chicago Medical Center. 293pTP cells were derived from HEK-293 cells as previously described [14]. HEK-293, 293pTP, and IOSE364 cells were cultured in Dulbecco's Modified Eagle Medium (DMEM) containing 10% fetal bovine serum (FBS, Gemini Bio-Products, West Sacramento, CA), 100 µg/ml streptomycin, and 100 U/ml penicillin. Human ovarian cancer lines were maintained in Roswell Park Memorial Institute (RPMI) 1640 or DMEM containing 10% FBS, 100 µg/ml streptomycin, and 100 U/ml penicillin. All cells were maintained in an incubator with 37°C and 5% CO<sub>2</sub>.

**Recombinant adenoviruses expressing BMP9, siBMP9, dnNotch1, GFP, and RFP construction and amplification.** Recombinant adenoviruses were constructed using AdEasy technology as previously described [15–18]. Recombinant adenoviruses overexpressing BMP9 (Ad-BMP9) and dominant-negative mutant Notch1 (AdR-dnNotch1) were kindly provided by T.-C. He, MD, PhD. from the University of Chicago Medical Center. For constructing AdR-siBMP9, three siRNAs of human BMP9 were made from Invitrogen's BLOCK-IT RNAi Designer program and simultaneously inserted into an adenoviral shuttle vector as previously described [19–21]. Analogous adenovirus expressing only GFP (Ad-GFP) or RFP (Ad-RFP) was used as a control [22–24]. 3–5 µg/ml polybrene was added to all adenoviral infections to potentiate infection efficiency.

**RNA isolation and touchdown quantitative reverse transcription polymerase chain reaction (TqPCR).** Total RNA from cells was isolated with TRIZOL reagent (Invitrogen, Carlsbad, CA) according to the manufacturer's instructions. RNA was reversely transcribed into cDNA

products using hexamer and M-MuLV Reverse Transcriptase (New England Biolabs, Ipswich, MA). The cDNA products were diluted 10–100 folds and served as PCR templates. PCR primers were designed by the Primer3 Plus program and used to amplify the target genes. TqPCR protocol was carried out as previously described [25]. Briefly, the SYBR Green (Bimake, Houston, USA) qPCR reactions were set up based on the manufacturer's instructions. TqPCR reaction was performed in triplicate as follow conditions: 95°C × 3 min for 1 cycle; 95°C × 20 s, 66°C × 10 s for 4 cycles reduced by 3°C per cycle; following 95°C × 20 s, 55°C × 10 s, 70°C × 1 s for 40 cycles. Gene expression levels were normalized to glyceraldehyde 3-phosphate dehydrogenase (GAPDH) followed by calculation using the 2<sup>-ΔΔCt</sup> method. The qPCR primer sequences are shown in Table 1.

**Western blotting.** Cultured cells were lysed by RIPA buffer with 1 mmol/l PMSF (Solarbio, Beijing, China). Protein concentrations were detected with the BCA kit (Boster Biological Technology, China). Equivalent proteins were separated on 8–10% gradient polyacrylamide gels electrophoretically and then transferred to the polyvinylidene difluoride (PVDF) membranes. The diluted primary antibodies were used to incubate the membranes overnight at 4°C, following the incubation with the peroxidase-coupled secondary antibodies for 1 h at 37°C. Proteins were visualized with the enhanced chemiluminescence reagents (Beyotime Biotechnology, Shanghai, China), and then quantified using VersaDoc Imaging System (Bio-Rad, CA, USA). The primary antibodies used were as follows: anti-NICD1 (sc-373891, Santa Cruz, USA), anti-BMP9 (sc-514211, Santa Cruz, USA), anti-β-Actin (sc-47778, Santa Cruz, USA). β-Actin was used as an internal control.

**Table 1. Primer sequences for qPCR.**

Primer (human)	Forward	Reverse
BMP9	CCTGGGCACAACAAGGAC	CCTTCCCTGGCAGTTGAG
Notch1	CCTGAGGGCTTCAAAGTGTC	CGGAACTTCTTGGTCTCCAG
Notch2	AAGCAGAGTCCCAGTGCCTA	CAGGGGGCACTGACAGTAAT
Notch3	CAACCCGGTGTACGAGAAGT	TGGAACGCAGTAGCTCCTCT
Notch4	CCATTGACACCCAGCTTCTT	CTGAACAGAAGTCCCGAAGC
Dll-1	GACTCGGGCTGTCAACTTC	CCTCCTCTTCCAGCAGCATT
Dll-3	GAGACACCCAGGTCCTTTGA	CAGTGGCAGATGTAGGCAGA
Dll-4	CGTCTGCCTTAAGCACTTC	GAATTTAAGGGCAGTTGGA
Jag1	AAGGGGTGCGGTATATTCC	GTTGACACCATCGATGCAAG
Jag2	TGATGACTTTGGTGGCAAGA	AGCCACTGTCACAGATGCAG
HEY1	GTGCTCCCTGTGGTCACC	GGGCTTGCCAAGGTTTGC
HES1	CGATGGCCAGTTTGCTTT	CCGCTGGAAGGTGACACT
HES2	CCAGCTTAAGGGGCTCATCC	CAGGAAGCGCACGGTCATTT
c-Myc	CGTCTGGGAAGGGAGAT	CGCTGCTATGGGCAAAGT
p27	AGATGTCAAACGTGCGAGTG	TCTCTGCAGTGCTTCTCCAA
MMP9	CCCGGACCAAGGATACAGT	GCCATTCACGTCGTCCTTA
Cyclin D1	TGTTTGAAGCAGGACTTTG	TGGACCAAAGGATTCTCTAA
GAPDH	CAACGAATTTGGCTACAGCA	AGGGGAGATTCAGTGTGGT

The quantitation analysis was determined by Image-Pro plus 6.0 software (Media Cybernetics, USA).

**WST-1 cell proliferation assay.** Cells in triplicate were seeded in the 96-well plate with  $1 \times 10^3$  cells/well after adenovirus infection and were cultured for 0 h, 24 h. Additionally, 30  $\mu$ l premixed WST-1 reagent (Clontech, Mountain View, CA, USA) was transferred into each well and incubated for 2–4 h. Finally, the absorbance at 450 nm was measured at the appointed time points with a microplate reader.

**Colony formation assay.** 200–400 cells/well were seeded into a 60 mm plate after adenovirus infection and incubated with 2% FBS medium for 10–14 days. Afterward, cells were washed gently with PBS once and stained with 0.5% Crystal Violet Staining Solution (Solarbio, Beijing, China) at room temperature for 20–30 min. Then washed, air-dried, and macrographic images were taken. Each assay was performed in triplicate. The quantitative analysis was determined by ImageJ software (National Institutes of Health, USA).

**Wound-healing assay.** Cells grew to the confluence with 10% FBS medium in 6-well cell culture plates. Subsequently, cells were wounded with sterile micro-pipette tips following the incubation in a serum-free medium. The wound healing status was recorded at the approximately same locations using a bright-field microscope for 0 h, 24 h. Each assay was performed in triplicate. The quantitative analysis was determined by ImageJ software (National Institutes of Health, USA).

**Cell cycle analysis.** Cells were plated in 6-well cell culture plates and infected with different adenoviruses. After 48 h,  $1 \times 10^6$  cells were harvested, fixed, and stained with Cell Cycle Analysis Kit (Beyotime Biotechnology, China) at 37°C for 30 min. The cell cycle was measured using flow cytometry (FACSCalibur, Becton Dickinson, USA). Data analysis was done with Modifit software. Each assay condition was performed in triplicate.

**Xenograft model.** SKOV3 cells were collected and resuspended in PBS after indicated adenoviral infection for 36–48 h.  $5 \times 10^6$  SKOV3 cells/tumor were inoculated subcutaneously into female athymic nude mice (5–6 weeks). After 3 weeks, the nude mice were sacrificed by CO<sub>2</sub> sealed. The masses were stripped from injection points. Tumor masses were weighed with an analytical balance. Volumes of tumor masses were measured using an external caliper and calculated using the equation  $(L \times W^2)/2$ . All animal experimental procedures were performed according to an Animal Care and Use Protocol approved by The University of Chicago Medical Center Institutional Animal Care and Use Committee and Ethics Committee of the First Hospital of Lanzhou University.

**Hematoxylin and eosin staining.** Retrieved tissues were fixed, decalcified in 10% formalin, and embedded in paraffin. The finished paraffin masses were sectioned and fixed on the slides, then stained with hematoxylin and eosin (HE, Sigma-Aldrich, MO, USA). The cover glass was fixed on the slide with 10% Neutral Balsam. The sections were made and then photographed using a microscope.

**Immunohistochemistry.** Paraffin-embedded tissues were cut into sections and performed antigen retrieval. Subsequently, sections were incubated with the primary antibody overnight at 4°C. After three washes with PBS, sections were incubated with moderated secondary HRP-conjugated antibody for 20 min at RT and counterstained with hematoxylin. For immunostaining analysis, a primary rabbit anti-PCNA (GTX100539, GeneTex, CA, USA) antibody was used.

**Statistical analysis.** All quantitative experiments were performed in triplicate. Data were analyzed with SPSS software and expressed as mean  $\pm$  standard deviation (SD). Statistical significances of all experiments were determined by one-way analysis of variance included an LSD post hoc test. A value of  $p < 0.05$  was considered statistically significant.

## Results

**BMP9 expression is increased in human OC cells and BMP9 promotes OC cell proliferation and migration *in vitro*.** We first detected the inherent expression of BMP9 in IOSE364 and OC cell lines (HeyA8, SKOV3, OVCAR3, OVCAR8, and CAOV3). We found that the expression of BMP9 was increased in human OC cell lines SKOV3, HeyA8, OVCAR3, and OVCAR8 ( $p < 0.001$ ), and has no difference compared CAOV3 cells with IOSE364 cells (Figures 1A, 1Ca). But the mRNA abundance of BMP9 in OC cell lines was low overall (Figure 1A). To investigate the function of BMP9 in OC cells, we used recombinant adenoviruses overexpressing BMP9 (Ad-BMP9) or silencing BMP9 (AdR-siBMP9), which infected OC cells with high efficiency. Furthermore, compared with the GFP control group, the Ad-BMP9 or AdR-siBMP9 infected OC cells exhibited a marked increase or decrease in BMP9 expression ( $p < 0.001$ ) (Figures 1B, 1Cb). We selected SKOV3 and OVCAR3 cells to further clarify the function of BMP9 in OC cells *in vitro*. We found that overexpression of BMP9 significantly promoted the cell proliferative viability of SKOV3 and OVCAR3 cells while silencing BMP9 remarkably inhibited the effect (Figures 1Da, 1Db). Moreover, the overexpression of BMP9 significantly accelerated SKOV3 cell migration, which was remarkably inhibited by the silencing of BMP9 (Figures 1Ea, 1Eb). Thus, we demonstrated that BMP9 promoted OC cell proliferation and migration *in vitro*.

**The inherent expression of Notch receptors and ligands exists in human OC cells.** We detected the inherent expression of Notch receptors (Notch1, 2, 3, and 4) and ligands (Dll-1, 3, 4, and Jag1, 2) in IOSE364 and human OC cell lines (HeyA8, SKOV3, OVCAR3, OVCAR8, and CAOV3). Compared with IOSE364 cells, the expression of Notch1, Notch2, Jag1, and Jag2 was remarkably increased in SKOV3 cells, and the expression of Notch1, Notch3, Dll-3, Jag1, and Jag2 was significantly elevated in OVCAR3 cells (Figures 2A, 2B). However, Notch 1–4 receptors have not been upregulated and Dll-3, Jag1, Jag2 ligands expression was elevated in the OVCAR8 cell line (Figure 2). Moreover, the expression of

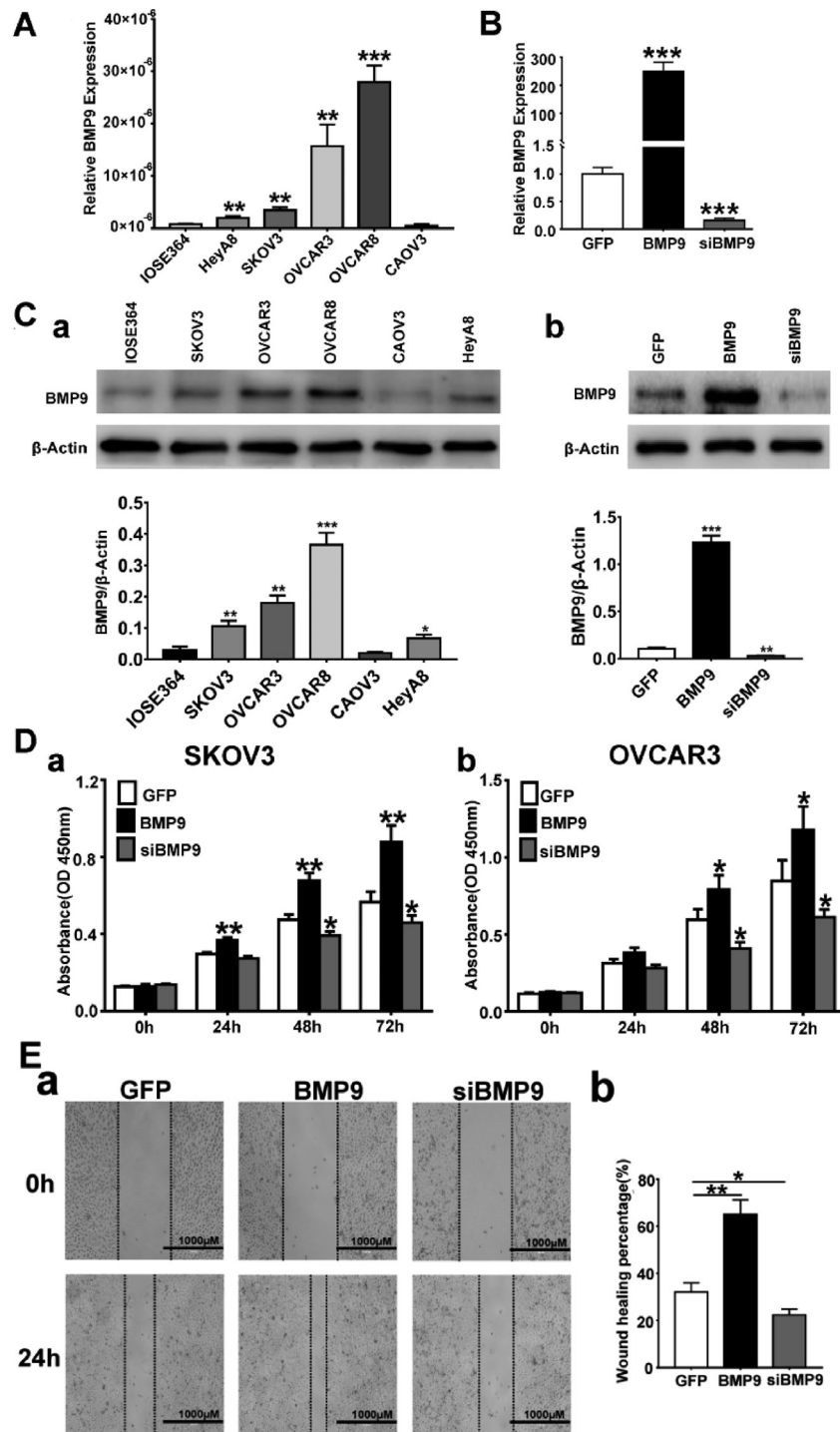


Figure 1. Endogenous BMP9 is increased in OC cells and BMP9 promotes OC cell proliferation and migration *in vitro*. A) The mRNA expression of BMP9 in SKOV3, HeyA8, CAOV3, OVCAR3, OVCAR8, and IOSE364 cells was measured by TqPCR assay. IOSE364 cells act as a control group. B) Ad-BMP9 and AdR-siBMP9 infected SKOV3 cells and the expression of BMP9 were verified by TqPCR assay. C) (a) The protein expression of BMP9 in SKOV3, OVCAR3, OVCAR8, CAOV3, HeyA8, and IOSE364 cells was measured by western blot. And the ratio of BMP9/β-Actin was quantified using Image-Pro Plus software. IOSE364 cells act as a control group. (b) Ad-BMP9, AdR-siBMP9, and Ad-GFP infected SKOV3 cells and the expression of BMP9 was verified by western blot. Image-Pro Plus software was used to quantify the ratio of BMP9/β-Actin. Each assay was performed in triplicate. \* p<0.05, \*\*p<0.01, \*\*\*p<0.001. D) The cell viability was assessed at the appointed time points by the WST-1 assay after SKOV3 and OVCAR3 cells were infected with Ad-BMP9, AdR-siBMP9, and Ad-GFP. GFP serves as a control. E) SKOV3 cells were infected with Ad-BMP9, AdR-siBMP9, and Ad-GFP. Cell migration was assessed by wound-healing assay. a) Cell migration area was measured at 0 h and 24 h by wound-healing assay. Scale bars, 1000 μm. b) ImageJ software was applied to quantitatively analyze the wound-healing areas. Each assay was done in triplicate. \*p<0.05, \*\*p<0.01, \*\*\*p<0.001

Notch3 receptor and Dll-3, Jag2 ligands was increased in the CAOV3 cell line (Figures 2A, 2B). The results showed that different Notch receptors and/or ligands might be expressed in human OC cells.

**BMP9 upregulates the expression of Notch1 and Jag2 and induces Notch1 intracellular domain (NICD1) accumulation.** In order to investigate the interaction cross-talk between BMP9 and Notch signaling in OC, SKOV3 cells were infected with adenoviruses overexpressing BMP9. We found that only Notch1 and Jag2 expression was significantly upregulated in the BMP9 group while the expression of other Notch receptors and ligands was downregulated compared with the GFP control group (Figure 3A). Furthermore, NICD1 was noteworthy increased in the BMP9 group compared with the GFP control group ( $p < 0.05$ , Figure 3B), suggesting that BMP9 activated the Notch1 signaling pathway. To effectively inhibit the Notch1 signaling pathway, we applied to dominant-negative Notch1 recombinant adenoviruses (AdR-dnNotch1), which was shown to infect SKOV3 cells with high efficiency (Figure 4A). The level of NICD1 was significantly decreased after infection with AdR-dnNotch1 in OC cells ( $p < 0.001$ , Figure 3C).

**BMP9 promotes OC cell proliferation through the Notch1 signaling pathway.** To further explore the function of BMP9 and Notch1 signaling in OC, we infected OC cells with high efficiency using Ad-GFP, Ad-BMP9, and/or

AdR-dnNotch1 (Figure 4A). BMP9 promoted OC cell proliferation by clone forming, which was reversed by the inactivation of Notch1 signaling (Figure 4B). Notably, we found that cell proliferation could be inhibited by AdR-dnNotch1 in SKOV3 and OVCAR3 cells (Figure 4B). The results were also demonstrated quantitatively by WST-1 assay ( $p < 0.05$ , Figure 4C). Thus, we demonstrated that BMP9 promoted OC cell proliferation through the Notch1 signaling pathway.

**BMP9-Notch1 signaling promotes cell cycle G1 to S/G2 progression in OC cells.** To further research the mechanism underlying BMP9-stimulated OC cell proliferation, we analyzed the effect of BMP9 and/or dominant-negative mutant of Notch1 signaling on OC cell proliferation using cell cycle assay. SKOV3 cells were infected with Ad-GFP, Ad-BMP9, and/or AdR-dnNotch1. As shown in Figures 5A and 5C, overexpression of BMP9 significantly increased the proportion of the S/G2 phase and decreased the proportion of the G1 phase in SKOV3 cells, which was reversed by

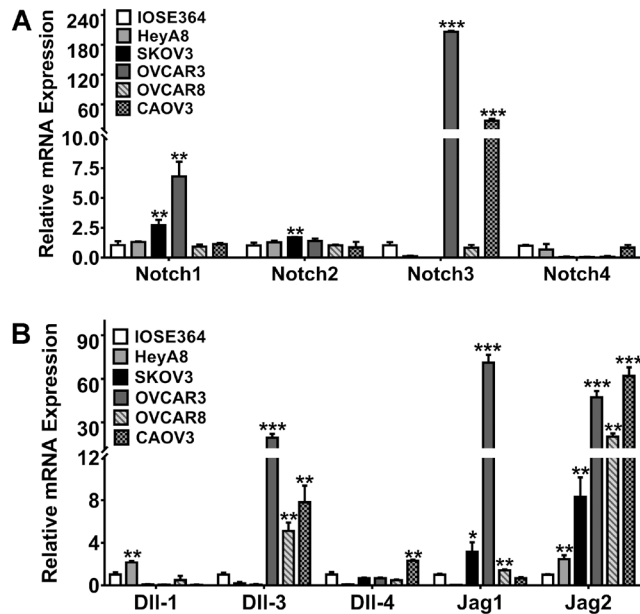


Figure 2. Notch receptors and ligands were expressed in human OC cells. (A) The mRNA expression of Notch receptors (Notch1, 2, 3, 4) in SKOV3, HeyA8, CAOV3, OVCAR3, and IOSE364 cells was measured by TqPCR assay. (B) The mRNA expression of Notch ligands (Dll-1, 3, 4, and Jag1, 2) in SKOV3, HeyA8, CAOV3, OVCAR3, OVCAR8, and IOSE364 cells was measured by TqPCR assay. IOSE364 cells act as a control group. Each assay condition was repeated three times. \* $p < 0.05$ , \*\* $p < 0.01$ , \*\*\* $p < 0.001$

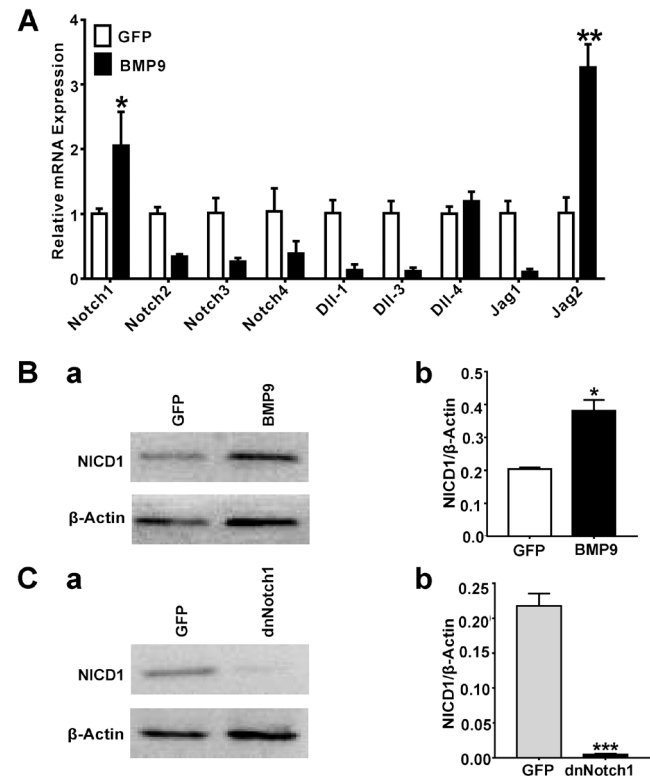
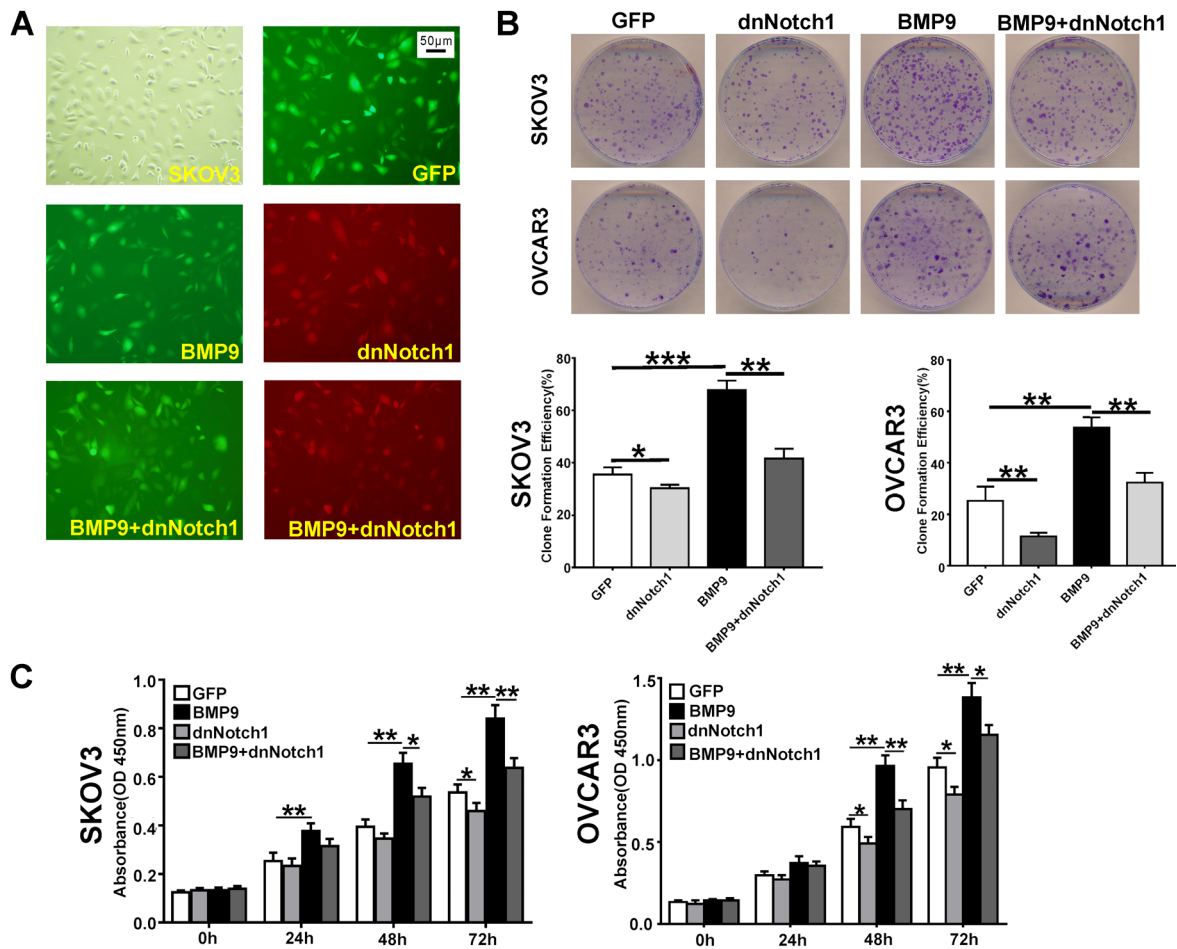


Figure 3. BMP9 activates Notch1 and Jag2 expression in OC cells and BMP9 induces NICD1 accumulation. (A) The mRNA expression of Notch receptors and ligands was detected using Ad-BMP9 and Ad-GFP infected SKOV3 cells by TqPCR assay. (B) The expression of Notch1 intracellular domain (NICD1) was detected by western blot assay (a) and the ratio of BMP9/ $\beta$ -Actin was quantified using Image-Pro Plus software (b). SKOV3 cells were infected with Ad-BMP9 and Ad-GFP for 72 h. GFP serves as a control. (C) NICD1 expression was verified by western blot (a). The ratio of NICD1/ $\beta$ -Actin was quantified using Image-Pro Plus software (b). SKOV3 cells were infected with Ad-GFP and AdR-dnNotch1 for 72 h. Each data was repeated three times. Images are shown representatively. \* $p < 0.05$ , \*\* $p < 0.01$ , \*\*\* $p < 0.001$



**Figure 4.** BMP9-Notch1 signaling accelerated OC cell proliferation *in vitro*. A) Recombinant adenoviruses expressing dominant-negative mutant Notch1 or overexpressing BMP9 transduce SKOV3 cells with high efficiency. Scale bars, 50  $\mu$ m. B) The cell proliferative viability was detected using a clone forming assay. Ad-GFP, Ad-BMP9, AdR-dnNotch1, Ad-BMP9+AdR-dnNotch1 infected SKOV3 or OVCAR3 OC cells, respectively. C) The cell viability was detected quantitatively by the WST-1 assay. Each data was repeated three times. Images were shown representatively. \* $p$ <0.05, \*\* $p$ <0.01, \*\*\* $p$ <0.001

inhibition of Notch signaling. Compared with the Ad-GFP group, the AdR-dnNotch1 group dramatically reduced the percentage of cells in the S/G2 phase and increased the percentage of cells in the G1 phase (Figures 5A, 5C). Thus, we demonstrated that BMP9 could effectively accelerate G1 to S/G2 progression in OC cells through the Notch1 signaling pathway.

**BMP9-Notch1 signaling accelerates OC cell migration.** To further explore the function of BMP9-Notch1 signaling in OC cells, we also analyzed OC cell migration. Using wound-healing assay, we found that Ad-BMP9 significantly promoted wound healing in SKOV3 cells ( $p$ <0.001, Figure 1D). AdR-dnNotch1-infected SKOV3 cells were shown to delay wound healing ( $p$ <0.05, Figures 5B, 5D). And BMP9-promoted SKOV3 cell migration was inhibited by AdR-dnNOTCH1 ( $p$ <0.001, Figures 5B, 5D). Therefore, these results indicated that the overexpression of BMP9

could accelerate OC cell migration through the Notch1 signaling pathway.

**BMP9-Notch1 signaling promotes subcutaneous tumor formation of OC cells.** We subsequently explored the effect of BMP9 on OC tumor growth *in vivo*. SKOV3 cells were infected with Ad-BMP9, Ad-BMP9+AdR-dnNotch1, AdR-dnNotch1, Ad-GFP and were injected subcutaneously into athymic nude mice. We found tumor masses in GFP, BMP9, and BMP9+dnNotch1 group. However, there was no subcutaneous tumor formation in the AdR-dnNotch1 group, suggesting that AdR-dnNotch1 inhibited OC tumor formation and growth. Compared with the GFP control group, the BMP9 group yielded larger tumor masses (Figure 6A), while the BMP9+dnNotch1 group yielded smaller tumor masses compared with the BMP9 group (Figure 6A). The result demonstrated that BMP9-promoted OC tumor growth was blunted by the inactivation of Notch1 signaling *in vivo*.

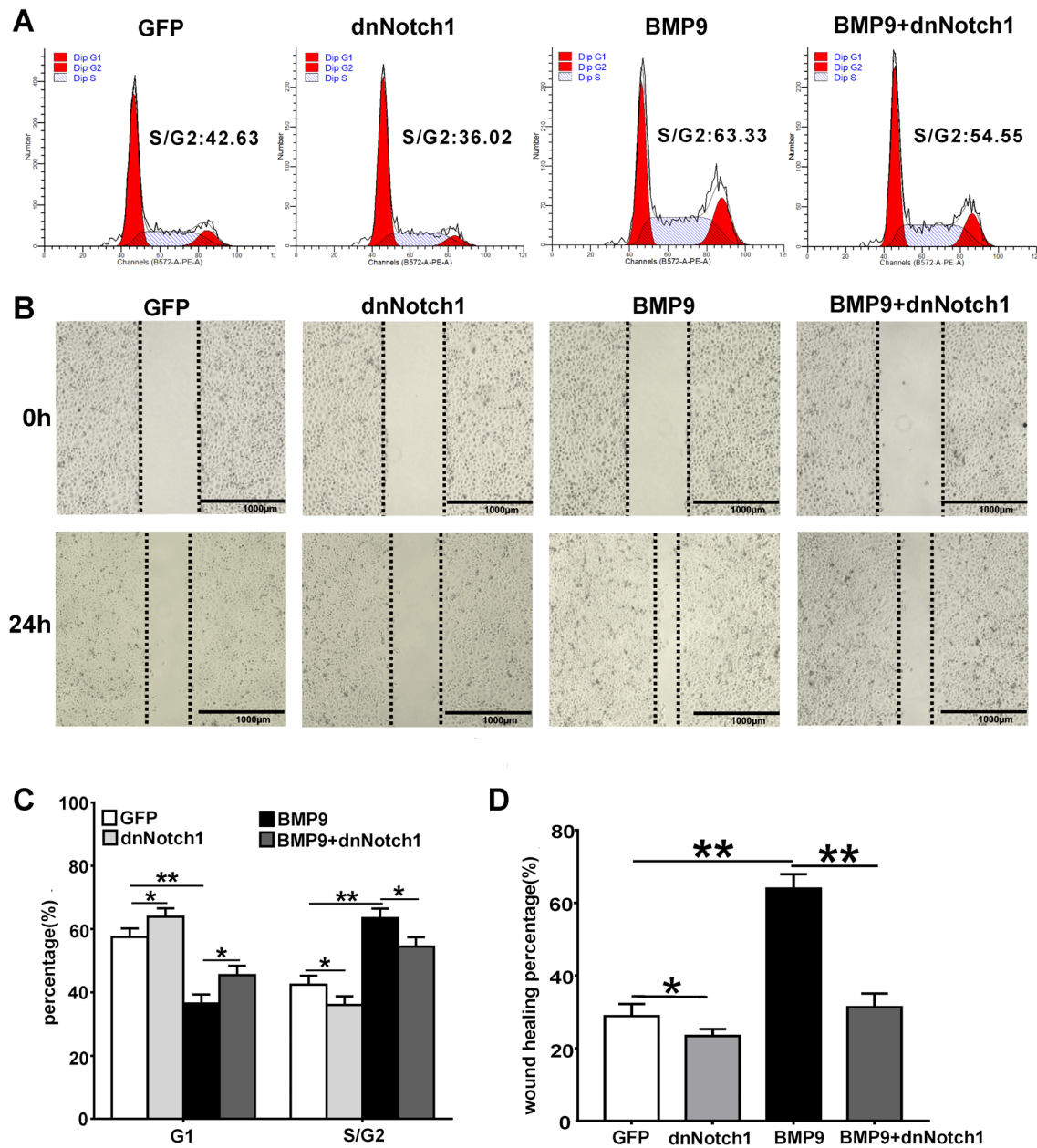


**Figure 5.** BMP9-Notch1 signaling promotes OC cell cycle G1 to S/G2 progression and cell migration *in vitro*. **A)** SKOV3 cells were infected with Ad-GFP, Ad-BMP9, AdR-dnNotch1, Ad-BMP9+AdR-dnNotch1 for 48 h. Cells were collected and treated with Cell Cycle Analysis Kit for flow cytometry analysis. The cell cycle in each group was measured by flow cytometry analysis. **B)** SKOV3 cells were infected with Ad-GFP, Ad-BMP9, and/or AdR-dnNotch1. Cell migration areas were measured at 0 h and 24 h by wound-healing assay. Scale bars, 1000  $\mu$ m. **C)** The percentages of G1 and S/G2 phase were performed quantitative statistics. **D)** ImageJ software quantitatively analyzed the wound healing areas. Each data was repeated three times. Images were shown representatively. \* $p < 0.05$ , \*\* $p < 0.01$ , \*\*\* $p < 0.001$

Quantitative analysis from tumor volume (Figure 6Ba) and tumor weight (Figure 6Bb) revealed that BMP9 remarkably promoted subcutaneous tumor formation, which was attenuated by inhibition of the Notch1 signaling. Subsequently, we further researched the structure of tumor masses. HE histologic staining showed morphological changes of subcutaneous tumor masses (Figure 6C). To clarify the effect of BMP9 on

OC subcutaneous tumor formation, we detected the expression of PCNA, which is a crucial cell proliferation marker, in mice xenograft tissues using immunohistochemistry. The BMP9 group had stronger PCNA staining compared with the GFP group (Figure 6C). The BMP9+dnNotch1 group showed weaker PCNA staining compared with the BMP9 group (Figure 6C). These findings revealed that BMP9 could

promote OC neoplasia and tumor growth *in vivo*, which was attenuated by inhibition of the Notch1 signaling. Collectively, these aforementioned results suggested that BMP9 promotes OC cell proliferation via the Notch1 signaling pathway *in vitro* and *in vivo*.

**BMP9-Notch1 signaling mediates the expression of HES2, c-Myc, Cyclin D1, MMP9, and p27 in OC cell growth.** To further identify the mechanism of BMP9-Notch1 signaling-promoted OC progression, we explored the expression of c-Myc, HES1, HES2, and HEY1 genes, which were involved in cell proliferation, cell fate determination [26]. These gene expressions were evaluated by a TqPCR assay. Compared with the GFP control group, the expression of c-Myc, HES2, and HEY1 was significantly downregulated in the dnNotch1 alone group ( $p < 0.05$ , Figures 7A–7C). Overexpression of BMP9 notably elevated c-Myc and HES2 expression, while the process was reversed by inhibition of the Notch1 signaling ( $p < 0.001$ , Figures 7A, 7B), suggesting that the expression of c-Myc and HES2 was mediated by the BMP9-Notch1 signaling pathway. To further explore the related genes mediated by BMP9 and Notch1 signaling, we tested the expression of MMP9, Cyclin D1, p27 genes using TqPCR assay. As shown in Figures 7D, 7E, and 7F, the inhibition of Notch1 signaling reduced MMP9 and Cyclin D1

expression as well as elevated p27 expression ( $p < 0.05$ ). And the overexpression of BMP9 significantly increased expression of MMP9 and Cyclin D1 but decreased p27 expression, which was reversed by the Notch1 signaling suppression ( $p < 0.05$ ). Collectively, the results suggested that BMP9 mediated the expression of HES2, c-Myc, MMP9, Cyclin D1, and p27 in OC cell progression through the Notch1 signaling pathway.

## Discussion

Ovarian cancer has the highest mortality among female malignancies [27, 28]. More than 90% of ovarian cancer originates from epithelial ovarian cancer (EOC) [1]. The overall five-year survival rate of EOC is under 45% [28]. Currently, research of ovarian cancer target therapy has attracted significant interest [6, 28]. To explore the potential therapeutic target, we detected BMP9 and Notch signaling expression in ovarian cancer cell lines. A previous study found BMP9 was mainly expressed in 25% of EOC tissue samples [8]. Although the mRNA expression abundance of BMP9 was quite low, we found the expression of BMP9 was significantly upregulated in OC cell lines compared with IOSE364 cells. Then we demonstrated that the overexpres-

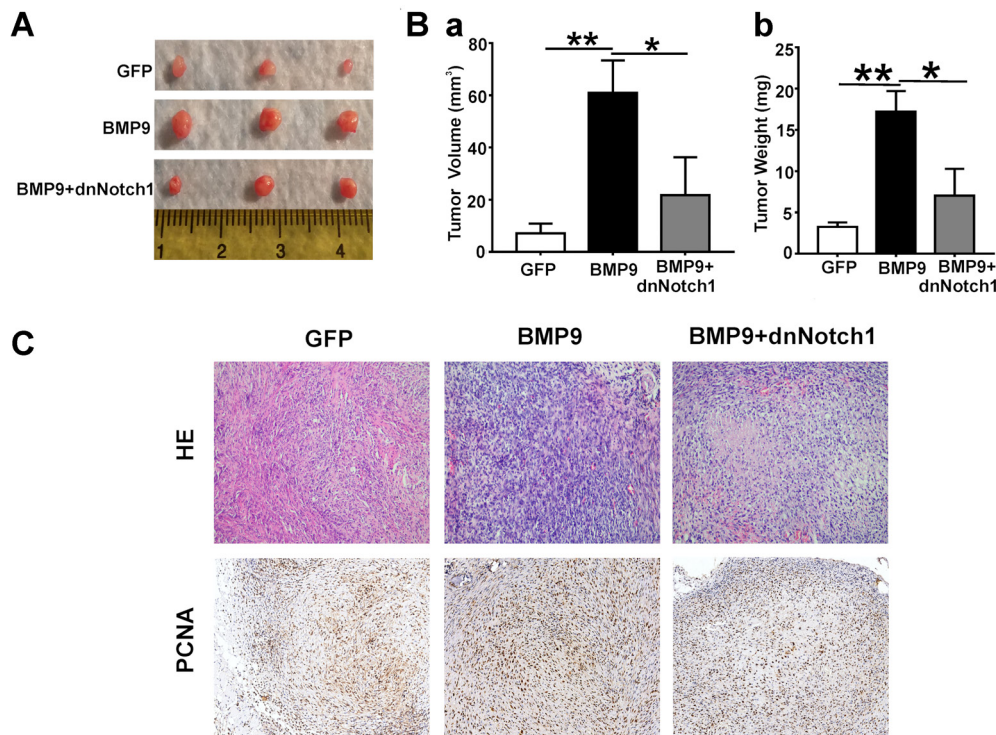


**Figure 6.** BMP9-Notch1 signaling promotes subcutaneous tumor formation of OC cells *in vivo*. SKOV3 cells were infected with Ad-GFP, Ad-BMP9, and/or Ad-dnNotch1. SKOV3 cells were subcutaneously injected into nude mice after being infected with different recombinant adenoviruses. A) Subcutaneous xenograft tumor formation of SKOV3 cells. B) Tumor volume (a) and tumor weight (b) were measured. C) Retrieved tumor samples were stained with HE staining (x200) and immunohistochemically stained with PCNA antibody (x200) to analyze the proliferative activity of OC tumor cells. Representative images are shown. \* $p < 0.05$ , \*\* $p < 0.01$ , \*\*\* $p < 0.001$

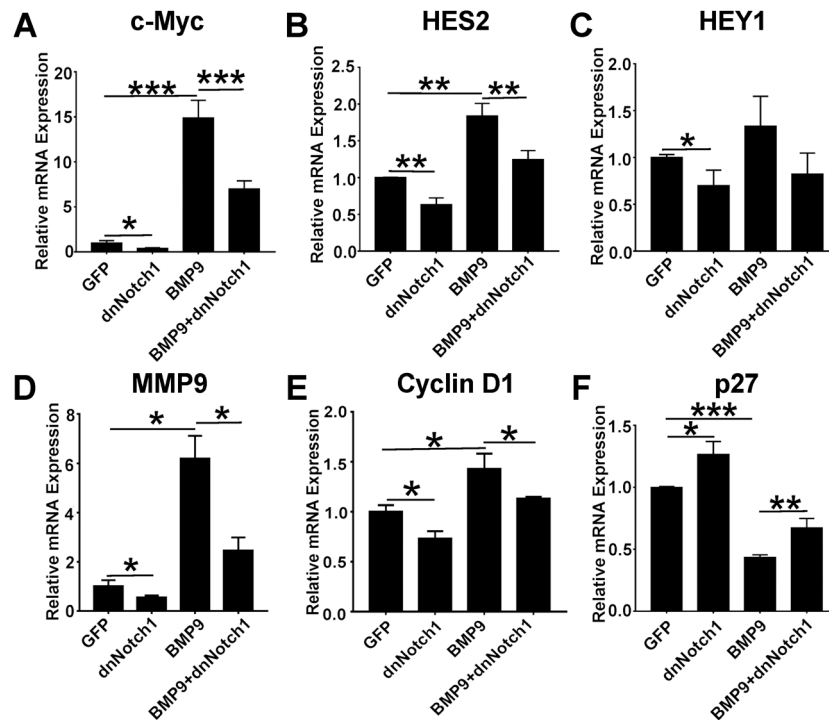


**Figure 7.** BMP9 regulates *c-Myc*, *HES2*, *MMP9*, *Cyclin D1*, and *p27* expression in OC progression through the Notch1 signaling. The expressions of *c-Myc* (A), *HES2* (B), *HEY1* (C), *MMP9* (D), *Cyclin D1* (E), and *p27* (F) genes were detected by TqPCR assay. SKOV3 cells were infected with Ad-GFP, Ad-BMP9, and/or AdR-dnNotch1. Each assay was performed in triplicate. \* $p < 0.05$ , \*\* $p < 0.01$ , \*\*\* $p < 0.001$

sion of BMP9 promoted OC cell proliferation and migration, and the BMP9 silencing inhibited the process. Besides, the overexpression of BMP9 induced Notch1 intracellular domain (NICD1) accumulation in OC cells. Subsequently, we demonstrated that BMP9 promoted OC tumor formation, cell proliferation, cell cycle progression, and migration, which was blocked by inhibition of the Notch1 signaling. Furthermore, BMP9-induced ovarian cancer cell progression also involved the elevation of *HES2*, *c-Myc*, *MMP9*, and *Cyclin D1* as well as repressed expression of *p27*. These findings indicate that the BMP9-Notch1 signaling may act as a potential intervention target in OC treatment.

Our research found that BMP9 potentiated OC tumor growth, cell proliferation, and migration through the Notch1 signaling using recombinant adenoviruses overexpressing or silencing BMP9. This is in line with research by Herrera et al. [8], which showed that BMP9 stimulated the proliferation of ovarian epithelial cells and OC cells in serum-starved conditions *in vitro* by knockdown of BMP9 and BMP9 reagent analysis. However, Varadaraj et al. [9] found that BMP9 did not promote ovarian epithelial cell proliferation. Previous research has confirmed that BMP9 is present at physiologically active in humans [29, 30] and bovine serum [29]. Herrera et al. [8] found that the proliferative effect had no difference between the BMP9 reagent group and the control group when ovarian epithelial cells and OC cells were

cultured in 5% FBS, suggesting that the expression of BMP9 stimulated by BMP9 reagent was masked by physiologically serum-derived BMP9, which had been identified by Herrera et al. [8]. Moreover, we found the inherent mRNA expression abundance of BMP9 is low in OC cell lines. This may be one of the reasons causing the aforementioned controversy. Accordingly, we constructed the overexpression of human BMP9 recombinant adenoviruses (Ad-BMP9) to further investigate the role of BMP9 in OC proliferation and migration. And we demonstrated that BMP9 overexpression notably promoted OC cell proliferation, cell cycle progression, cell migration, and tumor growth, which could be inhibited by the suppression of Notch1 signaling. Noteworthy, we found that solely the dnNotch1 group suppressed OC cell proliferation and migration compared with the GFP group *in vitro*. Besides, we confirmed that there was no measurable mass in the dnNotch1 group. And this result is consistent with the researches of Groeneweg et al. [10] and Rose et al. [11].

The mechanism of BMP9 in OC development remained unclear. According to the aforementioned results, we found that there are close connections between BMP9 and the Notch signaling in OC progression. Previously, Herrera et al. [8] found that BMP9 was involved in OC cell proliferation via the ALK2/Smad1/Smad4 pathway. Varadaraj et al. [9] suggested that BMP9 promoted ovarian cell anoikis via

the ALK3/ALK6/SMAD1/5 signaling *in vitro*. Given that BMP9 upregulated Notch1 and Jag2 in SKOV3 cells, we further demonstrated that the Notch1 signaling inhibition using AdR-dnNotch1 could blunt the BMP9-accelerated OC tumor growth, cell proliferation, cell cycle progression, and migration. Therefore, we thought it is essential for the interaction of BMP9 and the Notch1 signaling pathway in OC development. And Jag2 is considered to be a direct ligand of Notch1 in SKOV3 cells. Moreover, it is shown that the overexpression of BMP9 could significantly activate HES2, c-Myc, MMP9, and Cyclin D1 genes in OC cells, which was reversed by inhibition of the Notch1 signaling pathway. However, BMP9 could not activate HEY1 or HES1 (data not shown) in OC cells. The results validated that HES2 and c-Myc are downstream target genes of the BMP9-Notch1 signaling axis in OC cells. Cyclin D1 and MMP9 genes are cell cycle and cell migration marker genes, respectively [31, 32]. Overexpressing BMP9 upregulated MMP9 and Cyclin D1 genes, which were repressed by the Notch1 signaling inhibition. p27 is a nontypical tumor-inhibiting factor and mediates a number of processes including cell migration and cell cycle [33]. BMP9 overexpression downregulated p27 gene, which was reversed by dnNotch1. The results validated that BMP9 activated the Notch1-Jag2-HES2-c-Myc-Cyclin D1/MMP9/p27 axis, which promoted cell proliferation, cell cycle progression, and cell migration. In summary, our study reveals that BMP9 serves as a promoter in OC cell proliferation and migration, and participates in OC progression through the Notch1/Jag2/HES2/c-Myc signaling axis. The research deciphered the mechanism of the BMP9/Notch1/Jag2/HES2/c-Myc signaling in OC progression, through which BMP9 dramatically upregulated expression of Notch1 and Jag2 and induced NICD1 accumulation, thus regulating the downstream genes of c-Myc, HES2, MMP9, Cyclin D1, and p27 to accelerate OC progression. Our research clarifies the effect of BMP9 on OC progression and investigates a novel mechanism of the BMP9/Notch1/Jag2/ HES2 /c-Myc signaling in OC development.

**Acknowledgments:** The authors wish to thank T.-C. He, MD, PhD, from The University of Chicago Medical Center for his kind support and the provision of the adenoviral vectors used in the study. LY would also like to thank the members of the Molecular Oncology Laboratory at The University of Chicago Medical Center for their generous supports and valuable advice.

The reported work was supported by research grants from Key Laboratory of Gynecological Oncology of Gansu Province (18JR-2RA022) and Natural Science Foundation of Gansu Province (20JR-10RA693).

## References

- [1] NAORA H, MONTELL DJ. Ovarian cancer metastasis: integrating insights from disparate model organisms. *Nat Rev Cancer* 2005; 5: 355–366. <https://doi.org/10.1038/nrc1611>
- [2] MOUFARRIJ S, DANDAPANI M, ARTHOFER E, GOMEZ S, SRIVASTAVA A et al. Epigenetic therapy for ovarian cancer: promise and progress. *Clin Epigenetics* 2019; 11: 7. <https://doi.org/10.1186/s13148-018-0602-0>
- [3] ARVIZO RR, SAHA S, WANG E, ROBERTSON JD, BHATTACHARYA R et al. Inhibition of tumor growth and metastasis by a self-therapeutic nanoparticle. *Proc Natl Acad Sci U S A* 2013; 110: 6700–6705. <https://doi.org/10.1073/pnas.1214547110>
- [4] KOLONIN MG. Progenitor cell mobilization from extramedullary organs. *Methods Mol Biol* 2012; 904: 243–252. [https://doi.org/10.1007/978-1-61779-943-3\\_20](https://doi.org/10.1007/978-1-61779-943-3_20)
- [5] LI T, LI Y, GAN Y, TIAN R, WU Q et al. Methylation-mediated repression of MiR-424/503 cluster promotes proliferation and migration of ovarian cancer cells through targeting the hub gene KIF23. *Cell Cycle* 2019; 18: 1601–1618. <https://doi.org/10.1080/15384101.2019.1624112>
- [6] BAST RC JR, HENNESSY B, MILLS GB. The biology of ovarian cancer: new opportunities for translation. *Nat Rev Cancer* 2009; 9: 415–428. <https://doi.org/10.1038/nrc2644>
- [7] THÉRIAULT BL, NACHTIGAL MW. Human ovarian cancer cell morphology, motility, and proliferation are differentially influenced by autocrine TGFβ superfamily signalling. *Cancer Lett* 2011; 313: 108–121. <https://doi.org/10.1016/j.canlet.2011.08.033>
- [8] HERRERA B, VAN DINTHER M, TEN DIJKE P, INMAN GJ. Autocrine bone morphogenetic protein-9 signals through activin receptor-like kinase-2/Smad1/Smad4 to promote ovarian cancer cell proliferation. *Cancer Res* 2009; 69: 9254–9262. <https://doi.org/10.1158/0008-5472.CAN-09-2912>
- [9] VARADARAJ A, PATEL P, SERRAO A, BANDYOPADHAY T, LEE NY et al. Epigenetic Regulation of GDF2 Suppresses Anoikis in Ovarian and Breast Epithelia. *Neoplasia* 2015; 17: 826–838. <https://doi.org/10.1016/j.neo.2015.11.003>
- [10] GROENEWEG JW, FOSTER R, GROWDON WB, VERHEIJEN RH, RUEDA BR. Notch signaling in serous ovarian cancer. *J Ovarian Res* 2014; 7: 95. <https://doi.org/10.1186/s13048-014-0095-1>
- [11] ROSE SL, KUNNIMALAIYAAN M, DRENZEK J, SEILER N. Notch 1 signaling is active in ovarian cancer. *Gynecol Oncol* 2010; 117: 130–133. <https://doi.org/10.1016/j.ygyno.2009.12.003>
- [12] WANG M, WANG J, WANG L, WU L, XIN X. Notch1 expression correlates with tumor differentiation status in ovarian carcinoma. *Med Oncol* 2010; 27: 1329–1335. <https://doi.org/10.1007/s12032-009-9384-8>
- [13] SHAH MM, ZERLIN M, LI BY, HERZOG TJ, KITAJEWSKI JK et al. The role of Notch and gamma-secretase inhibition in an ovarian cancer model. *Anticancer Res* 2013; 33: 801–808.
- [14] WU N, ZHANG H, DENG F, LI R, ZHANG W et al. Overexpression of Ad5 precursor terminal protein accelerates recombinant adenovirus packaging and amplification in HEK-293 packaging cells. *Gene Ther* 2014; 21: 629–637. <https://doi.org/10.1038/gt.2014.40>
- [15] HE TC, ZHOU S, DA COSTA LT, YU J, KINZLER KW et al. A simplified system for generating recombinant adenoviruses. *Proc Natl Acad Sci U S A* 1998; 95: 2509–2514. <https://doi.org/10.1073/pnas.95.5.2509>

- [16] LUO J, DENG ZL, LUO X, TANG N, SONG WX et al. A protocol for rapid generation of recombinant adenoviruses using the AdEasy system. *Nat Protoc* 2007; 2: 1236–1247. <https://doi.org/10.1038/nprot.2007.135>
- [17] LEE CS, BISHOP ES, ZHANG R, YU X, FARINA EM et al. Adenovirus-Mediated Gene Delivery: Potential Applications for Gene and Cell-Based Therapies in the New Era of Personalized Medicine. *Genes Dis* 2017; 4: 43–63. <https://doi.org/10.1016/j.gendis.2017.04.001>
- [18] ZHANG B, YANG L, ZENG Z, FENG Y, WANG X et al. Leptin Potentiates BMP9-Induced Osteogenic Differentiation of Mesenchymal Stem Cells Through the Activation of JAK/STAT Signaling. *Stem Cells Dev* 2020; 29: 498–510. <https://doi.org/10.1089/scd.2019.0292>
- [19] WANG X, YUAN C, HUANG B, FAN J, FENG Y et al. Developing a Versatile Shotgun Cloning Strategy for Single-Vector-Based Multiplex Expression of Short Interfering RNAs (siRNAs) in Mammalian Cells. *ACS Synth Biol* 2019; 8: 2092–2105. <https://doi.org/10.1021/acssynbio.9b00203>
- [20] DENG F, CHEN X, LIAO Z, YAN Z, WANG Z et al. A simplified and versatile system for the simultaneous expression of multiple siRNAs in mammalian cells using Gibson DNA Assembly. *PLoS One* 2014; 9: e113064. <https://doi.org/10.1371/journal.pone.0113064>
- [21] LUO Q, KANG Q, SONG WX, LUU HH, LUO X et al. Selection and validation of optimal siRNA target sites for RNAi-mediated gene silencing. *Gene* 2007; 395: 160–169. <https://doi.org/10.1016/j.gene.2007.02.030>
- [22] YU X, CHEN L, WU K, YAN S, ZHANG R et al. Establishment and functional characterization of the reversibly immortalized mouse glomerular podocytes (imPODs). *Genes Dis* 2018; 5: 137–149. <https://doi.org/10.1016/j.gendis.2018.04.003>
- [23] ZHAO C, QAZVINI NT, SADATI M, ZENG Z, HUANG S et al. A pH-Triggered, Self-Assembled, and Bioprintable Hybrid Hydrogel Scaffold for Mesenchymal Stem Cell Based Bone Tissue Engineering. *ACS Appl Mater Interfaces* 2019; 11: 8749–8762. <https://doi.org/10.1021/acscami.8b19094>
- [24] ZHAO C, ZENG Z, QAZVINI NT, YU X, ZHANG R et al. Thermoresponsive Citrate-Based Graphene Oxide Scaffold Enhances Bone Regeneration from BMP9-Stimulated Adipose-Derived Mesenchymal Stem Cells. *ACS Biomater Sci Eng* 2018; 4: 2943–2955. <https://doi.org/10.1021/acsbmaterials.8b00179>
- [25] ZHANG Q, WANG J, DENG F, YAN Z, XIA Y et al. TqPCR: A Touchdown qPCR Assay with Significantly Improved Detection Sensitivity and Amplification Efficiency of SYBR Green qPCR. *PLoS One* 2015; 10: e0132666. <https://doi.org/10.1371/journal.pone.0132666>
- [26] ZHOU M, YAN J, MA Z, ZHOU Y, ABBOOD NN et al. Comparative and evolutionary analysis of the HES/HEY gene family reveal exon/intron loss and teleost specific duplication events. *PLoS One* 2012; 7: e40649. <https://doi.org/10.1371/journal.pone.0040649>
- [27] BRAY F, FERLAY J, SOERJOMATARAM I, SIEGEL RL, TORRE LA et al. Global cancer statistics 2018: GLOBOCAN estimates of incidence and mortality worldwide for 36 cancers in 185 countries. *CA Cancer J Clin* 2018; 68: 394–424. <https://doi.org/10.3322/caac.21492>
- [28] SOPIK V, IQBAL J, ROSEN B, NAROD SA. Why have ovarian cancer mortality rates declined? Part II. Case-fatality. *Gynecol Oncol* 2015; 138: 750–756. <https://doi.org/10.1016/j.ygyno.2015.06.016>
- [29] HERRERA B, INMAN GJ. A rapid and sensitive bioassay for the simultaneous measurement of multiple bone morphogenetic proteins. Identification and quantification of BMP4, BMP6 and BMP9 in bovine and human serum. *BMC Cell Biol* 2009; 10: 20. <https://doi.org/10.1186/1471-2121-10-20>
- [30] DAVID L, MALLET C, KERAMIDAS M, LAMANDÉ N, GASC JM et al. Bone morphogenetic protein-9 is a circulating vascular quiescence factor. *Circ Res* 2008; 102: 914–922. <https://doi.org/10.1161/CIRCRESAHA.107.165530>
- [31] JOHN RR, MALATHI N, RAVINDRAN C, ANANDAN S. Mini review: Multifaceted role played by cyclin D1 in tumor behavior. *Indian J Dent Res* 2017; 28: 187–192. [https://doi.org/10.4103/ijdr.IJDR\\_697\\_16](https://doi.org/10.4103/ijdr.IJDR_697_16)
- [32] KUNZ P, SÄHR H, LEHNER B, FISCHER C, SEEBACH E et al. Elevated ratio of MMP2/MMP9 activity is associated with poor response to chemotherapy in osteosarcoma. *BMC Cancer* 2016; 16: 223. <https://doi.org/10.1186/s12885-016-2266-5>
- [33] RAZAVIPOUR SF, HARIKUMAR KB, SLINGERLAND JM. p27 as a Transcriptional Regulator: New Roles in Development and Cancer. *Cancer Res* 2020; 80: 3451–3458. <https://doi.org/10.1158/0008-5472.CAN-19-3663>